

Raman scattering and photoluminescence properties of Ag doped ZnO nano particles synthesized by sol–gel method

B. Sathya¹ · D. Benny Anburaj¹ · V. Porkalai¹ · G. Nedunchezian¹

Received: 1 September 2016 / Accepted: 21 December 2016 / Published online: 6 January 2017
© Springer Science+Business Media New York 2017

Abstract Ag doped ZnO nanoparticles were synthesized through sol–gel technique. Hence, the synthetic approach provides a simple, easy, low cost effective and convenient route to obtain large quantities of Ag doped ZnO nanoparticles which were calcined at different temperatures (300, 350, 400 and 450 °C). The morphological studies, optical properties, phase purity and crystallite size were characterized by X-ray diffraction (XRD), scanning electron microscopy (SEM), energy dispersive X-ray spectrometry (EDAX), transmission electron microscope (TEM), ultra violet spectroscopy (UV), photoluminescence (PL), FT-Raman and atomic force microscopy (AFM) analysis. XRD patterns confirmed that the synthesized material is polycrystalline ZnO with hexagonal wurtzite structure and the average crystallite size varied from 17 to 11 nm. The optical band gap of the nanoparticles was tuned from 3.22 to 3.15 eV. The TEM study clearly shows the formation of nano spheres. Photoluminescence studies reveal that the Ag doped ZnO sample has the blue shift emission bands were observed. From the Raman spectrum all the peaks observed in samples matched with the Raman active modes of ZnO wurtzite structure.

1 Introduction

Nowadays, the metal oxide nano materials have more attention since their enormous potential in electronic and bio

sensor applications. ZnO is a n type semiconductor and has direct band gap of 3.37 eV at room temperature with a large exciton binding energy (60 meV) [1]. Zinc oxide (ZnO) is one of the II–VI semiconducting materials and it is a very promising material for semiconductor device applications [2]. In addition, it is biocompatible, bio-safe and phototoxic intracellular [3]. ZnO doped with transition metal (TM) ions, specify a number of applications in room temperature (RT) like nanolaser with n-type doping, p-type doping and RT ferromagnetic semiconductor nanomaterials [4]. Particularly, the nano structured ZnO is one of the important materials which is more attractive for the development of nano generators, solar cells, Light emitting devices (LEDs), spintronic, varistors, biological sensors, photonic devices and also used in data storage devices [5, 6]. In order to improve the optical, magnetic and electrical properties of ZnO nano particles, the dopants are added. Many reports are available that ZnO exhibits better photo catalytic activity in the presence of visible light when hybridized with noble metals such as Ag, Pt and Au etc [7].

The ZnO samples were doped with various elements like Ag, Al, F, Sn, In and Ga, by means of doping of ZnO, the orientation and morphology are modified either by thermal treatment or by the concentration variation and the type of dopants. The ZnO has various dopants in Group-Ib among possible acceptor dopants and silver is a good candidate for producing a shallow acceptor level in ZnO [8]. There is Good stability at high temperature and compatibility with other transparent conducting oxide (TCO) materials makes ZnO doped with Ag suitable for transparent and opto-electronic based technological applications. Ag could be a good candidate to improve luminescence efficiency [9].

So far, the doped ZnO nanoparticles have been prepared by various techniques such as sol–gel technique [10], soft

✉ D. Benny Anburaj
bennyburaj@gmail.com

¹ PG and Research Department of Physics, Thiru.Vi.Ka. Government Arts College, Thiruvarur, Tamil Nadu 610003, India

chemical route [11], co-precipitation method [12], hydrothermal method [13] and solvothermal method [14].

In the present work, properties of nanoparticles doped with Ag were prepared by sol–gel technique at different temperature, the mild change in optical band gap was observed. The optical properties were not affected by aging of parent solution. The surface properties, optical properties, microstructure and morphology play a significant role in the evolution of several devices, which are improved further for applications in optoelectronics and photocatalysts devices.

2 Experimental techniques

2.1 Synthesis process

The host precursor zinc acetate dihydrate ($Zn(CH_3COO)_2 \cdot 2H_2O$) were dissolved in deionized water, which was used as the starting solution (0.2 M). Silver nitrate ($AgNO_3$) were used as dopant precursors. The pH value of the starting solution was maintained at 9 by adding the required amount of NH_4OH solution. The reason for selecting pH as 9 are as follows [15] reported that keeping the $pH > 7$ leads to the formation of Zn–O bonds with enhanced crystalline quality. After, tri-ethanolamine ($C_6H_{15}NO_3$) was added as surfactant to control size and morphology of nano particles [16]. The resultant mixture was heated to 60 °C and magnetically stirred for 2 h. After completing the stirring process, the precipitate was separated carefully by filtration and washed several times with a mixture of ethanol and deionized water kept in the ratio of 1:3. The final product was irradiated with microwave oven (MS2042DW) for 30 min. Finally the powder calcined at 300, 350, 400, 450 °C for 2 h furnace.

3 Result and discussions

3.1 XRD characterization

The crystal structure and orientation of the Ag doped ZnO nanoparticles were investigated by X-ray diffractometer (PANalytical X’Pert Pro) engaging Cu- K_α radiation ($\lambda = 1.54056 \text{ \AA}$). Figure 1 showed as possibility of formation of Ag doped ZnO nano structure. The prepared ZnO nano particles were found to be polycrystalline in nature since there is no extra peak were found in the pattern. The diffraction peaks correspond to (1 0 0), (0 0 2), (1 0 1), (1 0 2), (1 1 0), (1 0 3), (1 1 2) and (2 0 1) planes were observed and intensity of these peak increases with increase of calcined at different temperatures. The additional peaks at $2\theta = 38^\circ, 44^\circ, 64^\circ$ were assigned to the (1 1 1), (2 0 0), (2

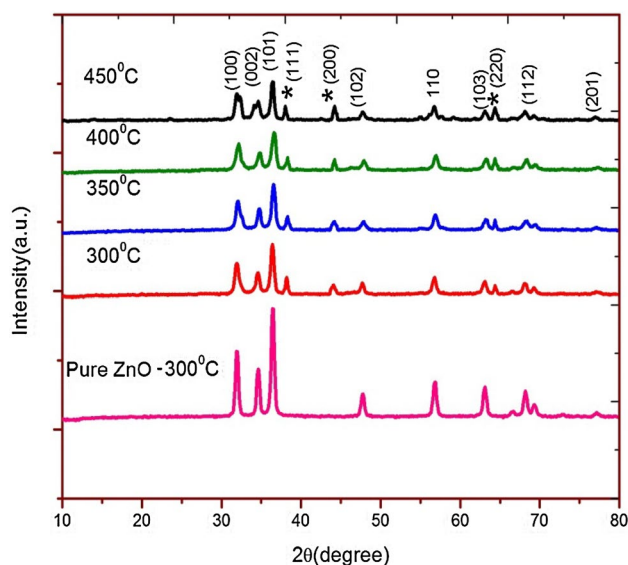


Fig. 1 XRD patterns Ag doped ZnO with different temperature

2 0) planes of silver ions. The planes confirm the formation of hexagonal wurtzite structure of ZnO for all the samples [17]. This observed XRD pattern is found to match with the JCPDS reference pattern 05-0664 and 04-0783 and confirms the hexagonal wurtzite structure with $P6_3mc(186)$ space group or C_{6v}^4 [18]. Diffraction peaks related to the impurities were not observed in the XRD pattern, confirming the high purity nature of the synthesized powder. The average crystallite size is calculated through Debye Scherer’s formula [19, 20].

$$D = k\lambda / \beta \cos \theta$$

where λ is the wavelength of Cu- K_α radiation (1.5406 Å), k is the shape factor (0.9), β is the full width at the half maximum (FWHM), θ is the Bragg’s diffraction angle.

The dislocation density (δ), which represent the amount of defect in the crystal, from the equation [21–23]

$$\delta = 1 / D^2$$

The resulting values of dislocation density are 3.27, 4.80, 5.35, 6.81, and 7.80. The average crystallite size range are 17.46, 14.42, 13.66, 12.11 and 11.54 nm in Table 1.

Table 1 XRD structural parameters of as prepared and calcined ZnO nanoparticles.

The presence of prominent peaks at (1 0 0), (0 0 2) and (1 0 1) showed the polycrystalline nature. Further the presence of very intensive peak in the XRD pattern confirms that, the calcined process affected the crystallinity ZnO nanoparticles positively and the crystalline quality increased at 450 °C. Added to this, Ag doping almost does not affect the position of the diffraction peak, but it strongly affects the peak intensity [24]. The Ag^+ ions in ZnO lattice behave as monovalent dopant, which have ability to

Table 1 XRD structural parameters of as prepared and calcined ZnO nanoparticles

Sample	Crystallite (nm)	Dislocation density $\delta \times 10^{-3}(\text{nm}^{-2})$
Pure ZnO	17.46	3.27
300 °C	14.42	4.80
350 °C	13.66	5.35
400 °C	12.11	6.81
450 °C	11 0.54	7.50

occupy both the lattice and interstitial sites due to higher ionic radius of Ag^+ ions (1.26 Å) than Zn^{2+} (0.74 Å) [25].

Figure 2 shows the variation of crystallite size of ZnO nanoparticles with temperature. From the graph it is observed that, when the calcined temperature is increased from 300 to 450 °C, the crystallite size could be decreased gradually. From this observation it can be inferred that, the crystal size is reduced at 450 °C calcined temperature due to the chemical strain produced by the thermo-mechanical forces. Simultaneously, the dislocation density is found to be increased.

3.2 Optical studies

The optical absorption spectra were taken for of pure and Ag doped ZnO particles calcined at various temperatures 300, 350, 400 and 450 °C respectively. The energy gap of the nanoparticles is estimated using the absorption edge and the band gap and it is found to be for pure ZnO is 3.22 eV. It varies from 3.20 to 3.15 eV at the interval of calcined temperatures from 300 to 450 °C which are summarized in Table 2. In the present particles, the optical

Table 2 Optical band gap of pure ZnO and calcined with different temperatures

Sample	Band gap (eV)
Pure ZnO	3.22
300 °C	3.20
350 °C	3.19
400 °C	3.17
450 °C	3.15

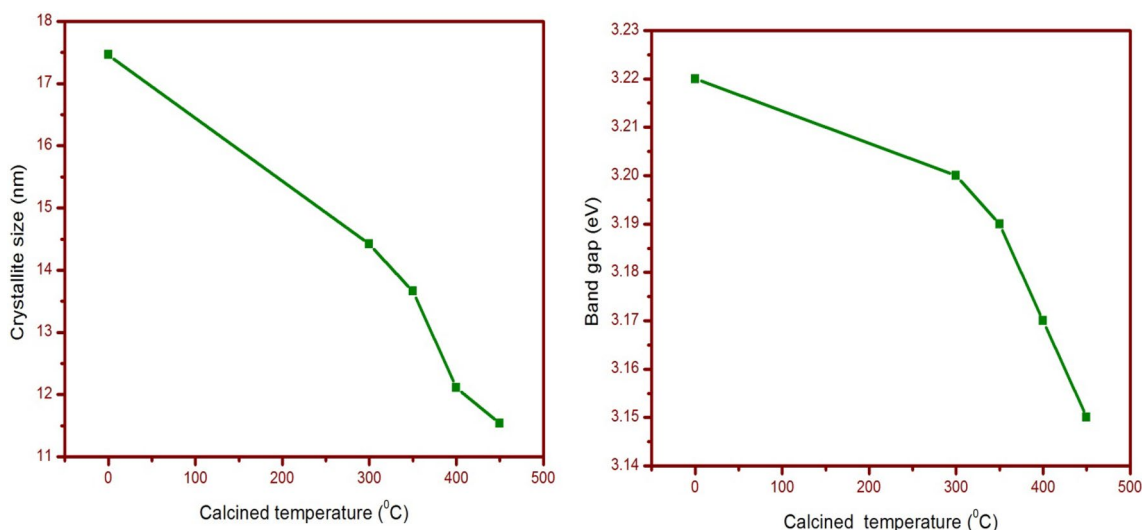
absorbance is low in the wavelength region of 400–700 nm. So it could be concluded that, the optical activity of the ZnO nanoparticles is low. Figure 3 shows the plots between $(\alpha h\nu)^2$ and photon energy ($h\nu$) for prepared and calcined ZnO nanoparticles.

Figure 4 shows the optical absorption estimates the optical activity of the compound. The optical band gap of ZnO was determined by extrapolating the linear portion of the curve from the plot of $(\alpha h\nu)^2$ versus $h\nu$. The optical band gap energy was determined using the formula [26].

$$\alpha h\nu = A (h\nu - E_g)^n$$

where α is the absorption co-efficient (m^{-1}), $h\nu$ is the photon energy (eV), A =constant, $n=1/2$ allowed direct transition, $n=2$ allowed indirect transition respectively. The intercept of this plot on the energy axis gives the energy band gap of the samples.

When Ag atoms doped with ZnO, the Ag atoms occupies the zinc site in the ZnO lattice while reducing the band gap of ZnO doped with acceptor [27]. Decreasing the band gap can be related to the presence of p-type conductivity in the silver doped ZnO nanoparticles. Silver doping in ZnO

**Fig. 2** Variation of average crystallite size and band gap of ZnO: Ag samples at different calcined temperature

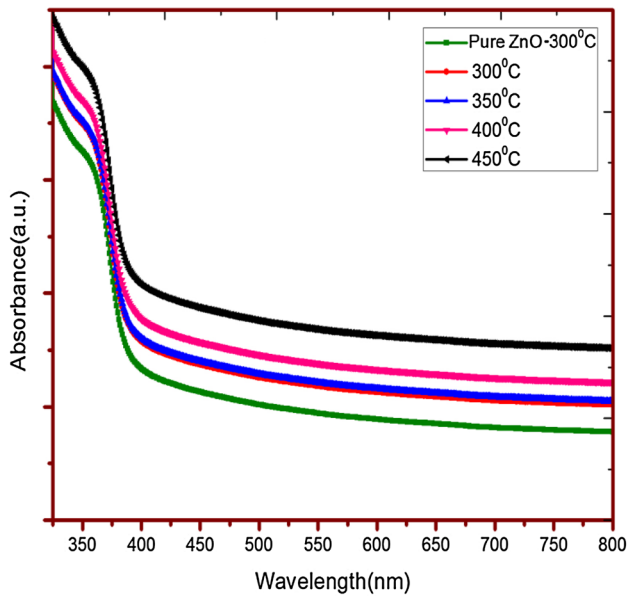


Fig. 3 UV absorption spectrum of ZnO: Ag nanoparticles at different temperature

provides the impurity band in the energy gap, which could be due to the formation of the p-type in the substance. Such a widening of band gap is known as Burstein-Moss shift [28] also called as blue-shift. This blue shift imposed the structural disorder of ZnO nanoparticles due to Ag-doping.

3.3 UV-transmittance analysis

Figure 5 shows the transmittance spectra of the as prepared and calcined ZnO nanoparticles. The transmittance

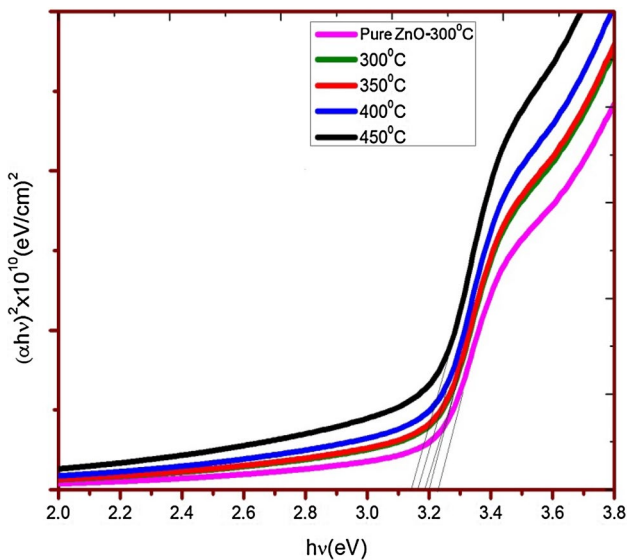


Fig. 4 Tauc plots of pure and Ag doped ZnO nanoparticles

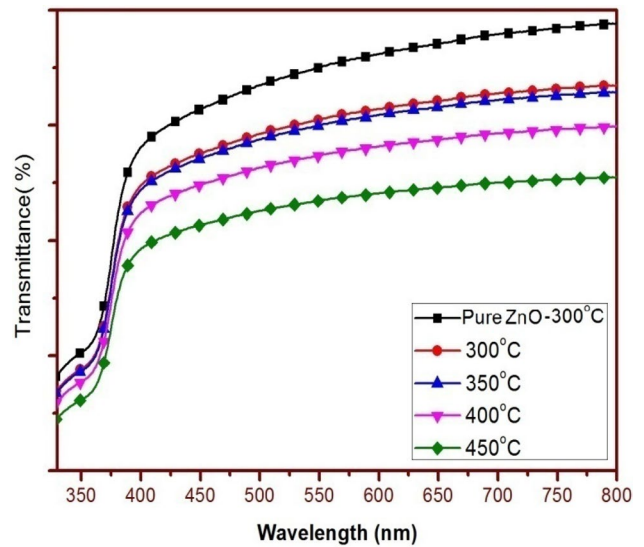


Fig. 5 Optical transmittance spectrum of Ag doped ZnO nanoparticles calcinated at different temperature

values of calcined ZnO nanoparticles are found to be higher than the particles are prepared at different temperatures. Hence, the transmittance value is further increased continuously with increasing calcined temperature. The transmittance value of ZnO nanoparticles calcined at 450 °C is 80% which indicate that, the particles at 450 °C yielded good transmittance. This implies that the particles have best structural and optical properties [29].

3.4 SEM analysis

Figure 6 the SEM micrographs of the surface of ZnO nanoparticles and different calcined temperatures. From the Fig. 6(a, b, c, d) one can find that, the microstructure consisted of many sphere shaped crystalline particles [30]. The microstructure formed is found to be uniform and compact structure which are interconnected by grains. These results suggested that, the size of the grains is large at low temperatures less than 350 °C. Further, it is reduced, when the temperature is increased. Thereby, the best uniform surface morphology is identified at 450 °C. However, the overall observation is that, the grain size is decreased and its surface becomes optically flat with increase the calcined temperature. However, this trend is the same as that of XRD results, which also showed the reduced crystallite size with increasing of calcined temperature.

If the size of the dopant and doping atoms are equal, the doping atoms can be positioned at the lattice sites. In this case, the ionic radius of Zn²⁺ and Ag⁺ is 0.74 and 1.29 Å respectively [31].

Fig. 6 SEM image Ag doped ZnO nanospheres **a** 300 °C, **b** 350 °C, **c** 400 °C and **d** 450 °C

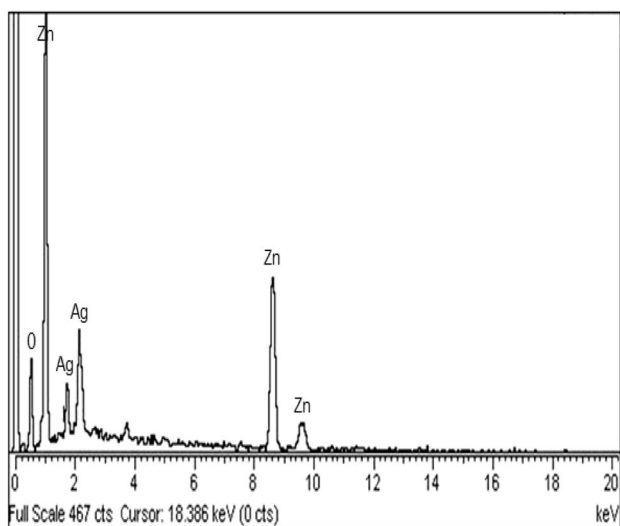
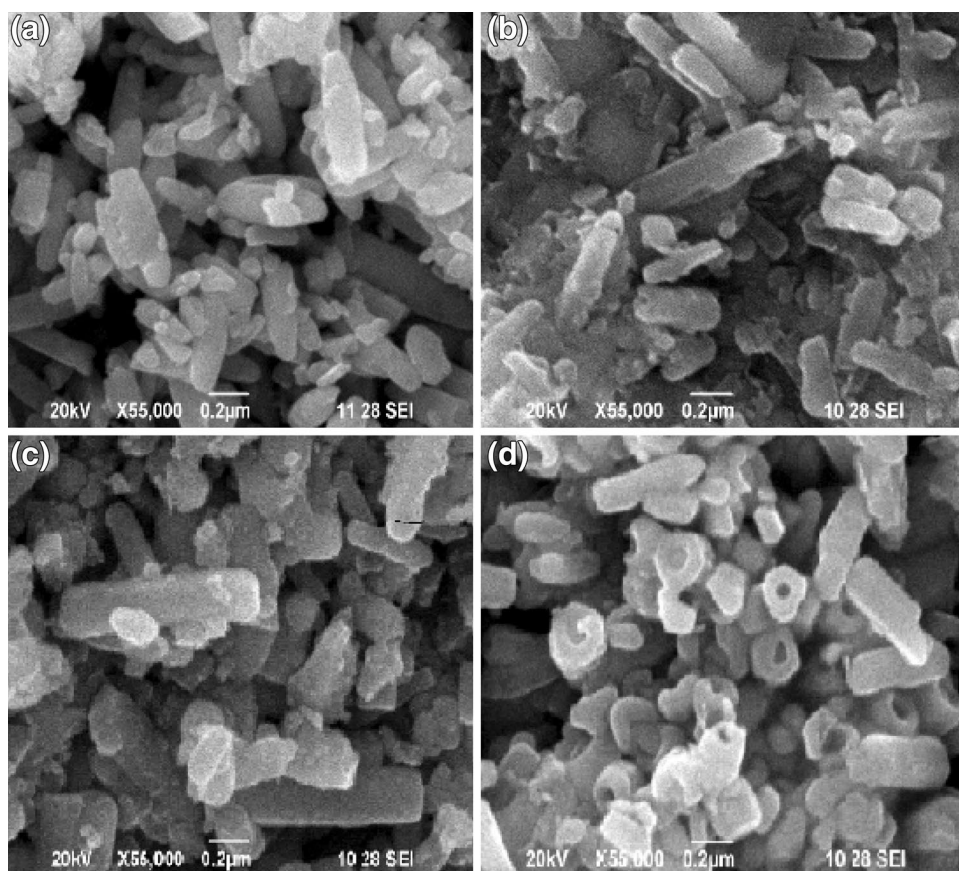


Fig. 7 EDAX spectrum of Ag doped ZnO nanoparticles

3.5 Elemental analysis by EDAX

The EDAX generated data consist of spectra showing peaks corresponding to the elements making up the true composition of the sample being analysed. The recorded energy

dispersive X-ray spectrum (EDAX) of ZnO nanoparticles at 450 °C is shown in Fig. 7. The EDAX spectrum exhibited clear peaks corresponding to Ag, Zn and O. The percentages of Ag, Zn and O elements of ZnO nanoparticles are 5.17, 46.34 and 48.49 mass %, respectively. From the modulated EDAX spectrum, it is very important to note that, the prepared ZnO is pure and free from the contamination. When the ZnO nanoparticle is calcined at 450 °C, it is very close to the stoichiometric compound [32].

3.6 AFM morphological studies

The 2D and 3D morphological view of the ZnO nanoparticles calcined at different temperatures as shown in Fig. 8. In this case, the influence of the calcined process over the surface morphology of the ZnO nanoparticles can be observed. The (3D) images of different morphologies are recorded with respect to calcined temperature 300–450 °C respectively [33].

3.7 TEM analysis

Figure 9 shows that the clear structural morphology and average particle size of the silver nanoparticles could be determined by TEM and SAED pattern. Figure 9 shows

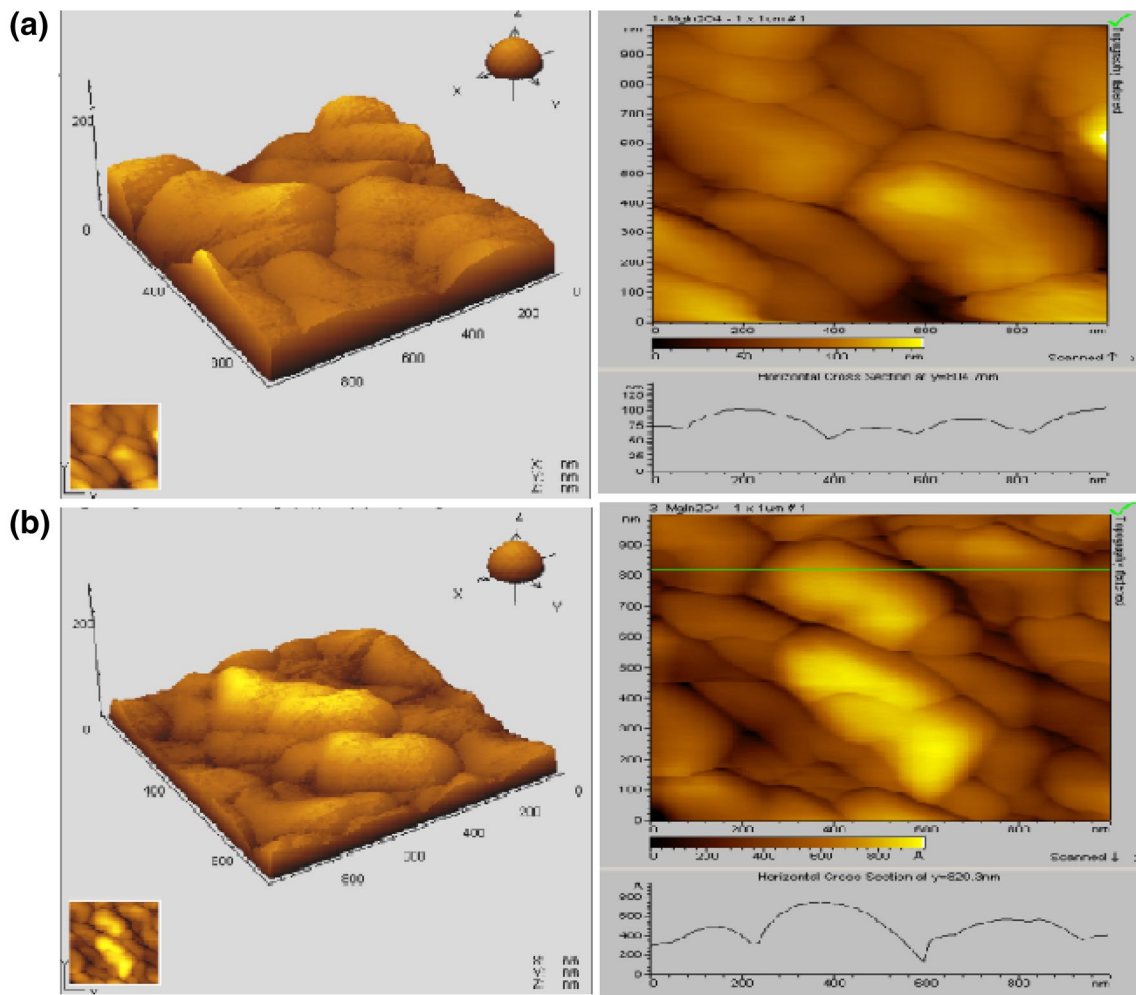


Fig. 8 AFM image of the Ag doped ZnO nanoparticles

the TEM high resolution images of ZnO nanoparticles and calcinated Ag doped ZnO nanoparticles. In the case of prepared ZnO nanoparticles as well as calcinated at 300 °C, it is found that, the particle size is large and nano-particle aggregates were seen very clearly. At 350–400 °C, the particle sizes are reduced and the Zn, Ag and O particles are coupled with one another and the nanospheres shape is produced. At 450 °C, each and every particle can be viewed and the particle size variation is found to be in the range from 28 to 12 nm. When the temperature is raising from 300 to 450 °C [34].

The clear information can be studied by taking the SAED images for the compound. Figure 10a, b showed the SAED pattern of ZnO nanoparticles calcinated at various temperatures 300 and 450 °C respectively. In Fig. 10a, the circular white patches are identified in the field of view which shows that the nano crystalline particles [35].

Figure 10b Contained dots and diffused concentric diffracted rings which obviously shows that the perfect crystallization of ZnO nanoparticles. The spots could be indexed corresponding to the reflections from the diffraction planes of (0 0 2), (1 0 0) and (1 0 1) of ZnO nanoparticles which is in accordance with the XRD results [36]. The SAED pattern of the ZnO nanoparticles calcinated at 450 °C also showed a dense and well defined granular structure, which extended throughout the end of the particles. The SAED pattern is composed of a series of rings with spots, which ensure that, these granular structures have nano-sized crystallites and the complete crystallization is formed at these temperature.

3.8 Raman spectra

Raman Spectra of Ag doped ZnO nanoparticles as shown in Fig. 11a–e. The intense peaks correspond to the formation

Fig. 9 TEM micrographs image of Ag doped ZnO nanoparticles

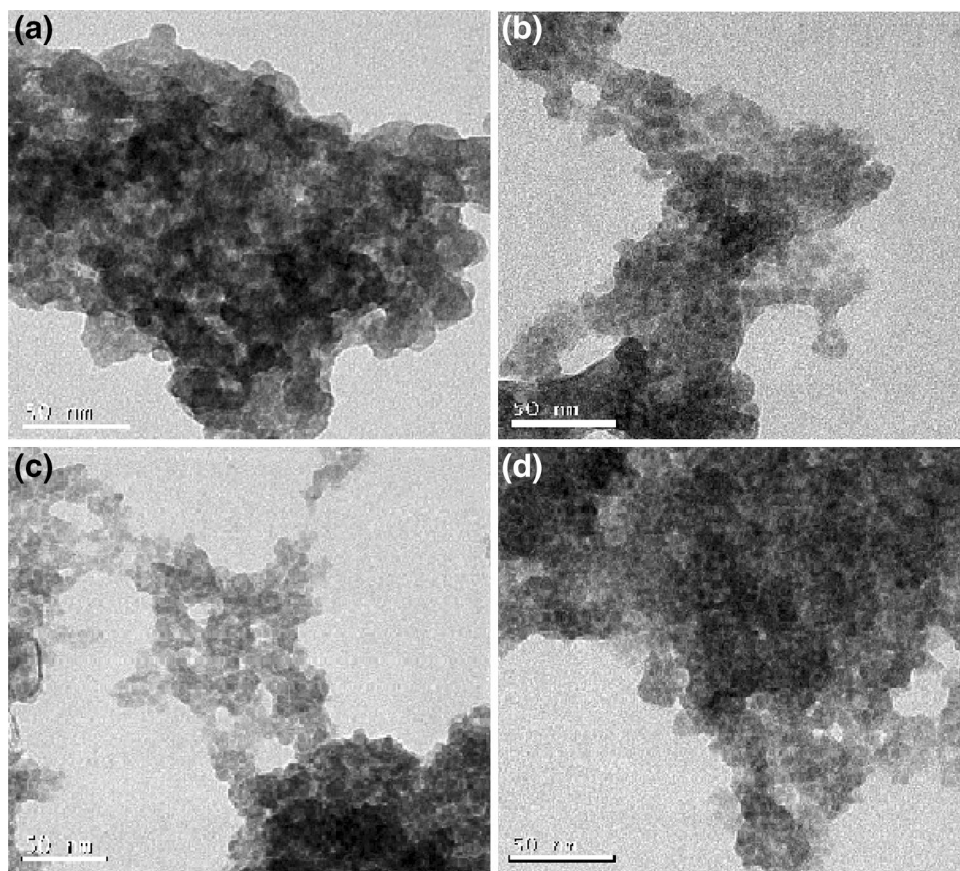
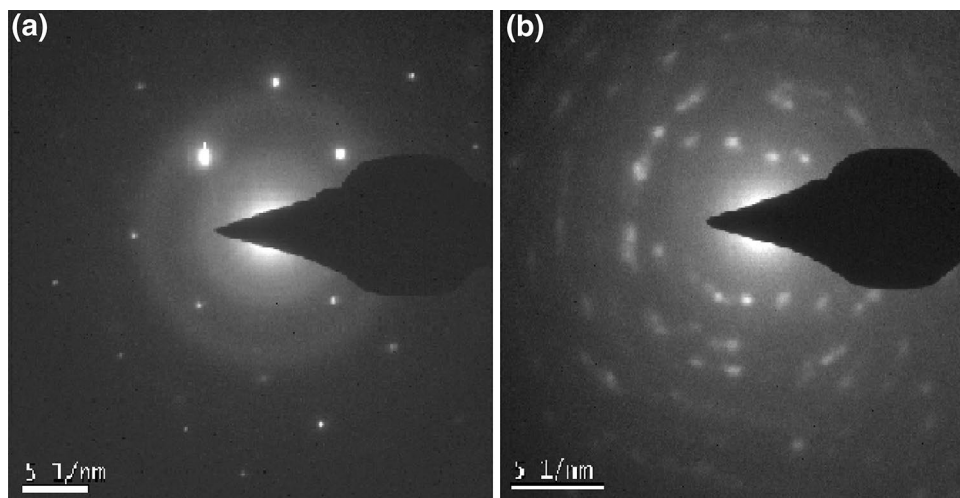


Fig. 10 SEAD pattern of Ag doped ZnO nanoparticles



of perfect crystallized particles. The broad peaks confirm the presence of nano crystallites ZnO particles. The structure of ZnO belongs to the C_{6v} symmetry group. In this case optical phonon branches could be represented by an equation.

$T_{opt} = A_1 + 2B_1 + E_1 + 2E_2$ which predicts two A_1 , two E_1 , two E_2 and two B_1 modes. Among these, A_1 and E_1

modes are polar and split into transverse (TO) and longitudinal optical (LO) phonons, all being Raman and infrared active. E_2 modes are only Raman active, and B_1 modes are infrared and Raman inactive (silent modes). Figure (a) shows the Raman spectra of as prepared ZnO nanoparticles. The modes that were observed at $459\text{ cm}^{-1}E_1$ (TO), 557 and 797 cm^{-1} , E_2 (low)– B_1 (high),

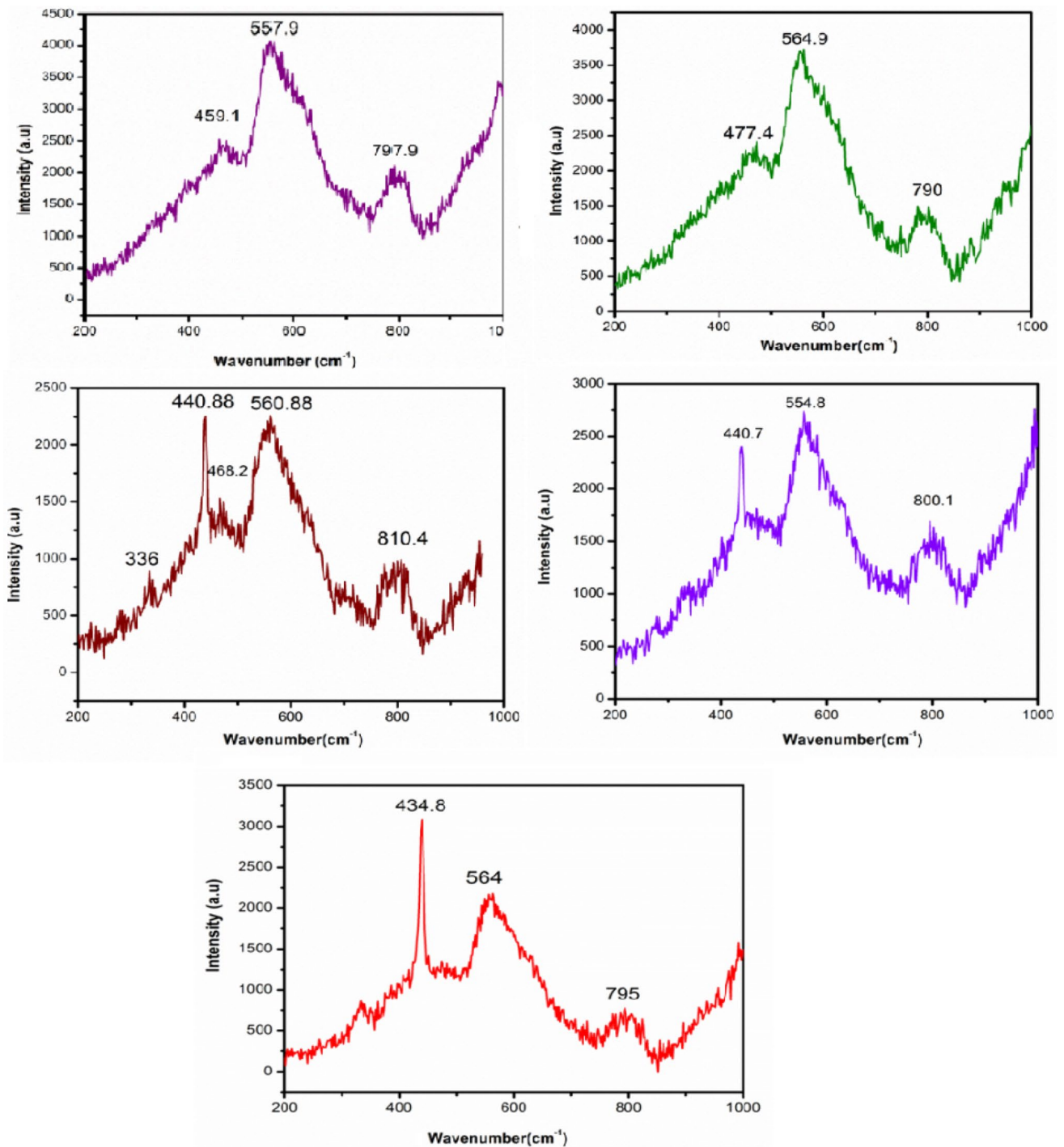


Fig. 11 Raman spectra **a** Pure ZnO, **b** Ag doped ZnO nanoparticles at different calcined temperatures

respectively. For all Ag doped ZnO and the 459,477, 440,468 and 434 cm⁻¹ modes correspond to E₂ mode of hexagonal wurtzite ZnO showing a very sharp feature. The 557, 564, 560, 554 cm⁻¹ peaks of E₁ (LO) mode corresponds to well resolved Raman peaks arising due to multiphonon and resonance processes and are related to oxygen deficiency [37].

The same tendency was not observed in ZnO at 450 °C samples and it has the maximum intensity peak at 434 cm⁻¹, and shows that the crystalline quality of this particle had been largely improved and also it contains very small crystallites as observed from the TEM images [38].

At, pure ZnO [38] the three Raman modes are observed at 459, 557 and 797 cm⁻¹. These peaks are assigned to A₁,

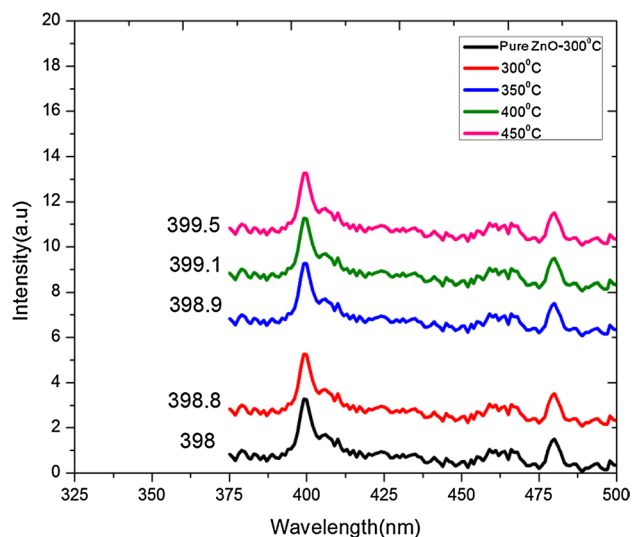


Fig. 12 PL spectra of Ag doped ZnO nanoparticles

E_1 , and E_2 modes. Such three vibrational peaks are assigned to each one mode of allowed transitions. Such these signals are observed at 477, 564 and 790 cm^{-1} respectively for Ag doped ZnO calcined at 300 °C. These vibrational bands moved up to the higher wavenumber region in increasing the calcined temperature from 300 to 450 °C. Due to this reason, further the crystallite size is reduced and force constant is increased between the bonds of the atoms (Zn–O and Ag–O) [39].

3.9 Photoluminescence analysis

The photoluminescence analysis used to analyze alloy inhomogeneities and variations in impurity concentration and calcined temperature. Figure 12 shows the recorded PL spectra of as prepared and calcinated ZnO nanoparticles. The excitation wavelength was found to be 398–399 nm. The PL peak of ZnO nanoparticles at 450 °C is observed at 399.5 nm. Whereas the peaks of Ag doped ZnO with calcined temperature 300 to 450 °C, are observed in the range of 399.5–398 nm. From this result, it is clear that the PL peak is shifted little bit from higher region of photon energy to lower photon energy region with increasing of calcined temperature. There is a small change in slightly shifted toward higher wavelength side. The first emission is due to recombination of holes and electrons present in valence and conduction bands [40]. This observation indicates that, the occurrence of blue shifts in the UV region due to Burstein-Moss effect [41]. This is mainly due to the displacement of Fermi level towards the conduction band in the ZnO material which also leads to the widening of band gap. The pointed out the photo luminescence peak with minimum intensity observed from about 300 to 700 nm depends on

the calcined temperature of ZnO nanoparticles. In general, the visible emissions are related to several intrinsic defects in ZnO NPs, which contains Zn vacancies (V_{Zn}), oxygen vacancy (V_{O}), Zinc interstitial (Zn_i), interstitial O (O_i), substitution of O at Zn position (O_{Zn}) and complex of V_{O} and Zn_i ($V_{\text{O}}\text{Zn}_i$) [39].

The emission spectra for the Ag-doped ZnO nanoparticles showed a broad spectral region of 375–500 nm which is composed of different peaks 398 and 399.5 nm. The incorporation of Ag apparently results a competitive phenomenon of blue–green (450–560 nm) PL emission [42]. This behaviour could be originated by more favourable transmission between the localized states generated by the Ag dopant or it could be due to the reduction of self-activated centers by occupation of Ag ions in the Zn vacancies [40].

4 Conclusion

The silver doped ZnO nanoparticles with nano grains have been synthesized by sol gel method. The nanoparticles were characterized by XRD, SEM, TEM, AFM and PL studies and their results are tabulated and also their variations are represented by the graph. The ZnO nano particles calcined at 300–450 °C showed preferential orientation of nanoparticles. The SEM analysis evidenced that the uniform sphere structures with decreasing grain size at higher calcined temperature. The influence of Ag doping over the surface morphology of the particles were observed and the grain size was found to be decreased with the incorporation of Ag. In optical study, it was observed that, the values of optical band gap changed (3.22–3.15 eV) with increasing of temperature. In the visible region, entire nano materials are acting as highly transparent (more than 80%). The TEM results showed a well crystallized nano structure of Ag doped ZnO nanoparticles. The PL emission peaks intensities can be varied from the region. The results suggest the future improvement of luminescence efficient materials at low temperatures with Ag doped ZnO nanostructures using on the photoalytic devices.

References

1. K. Saravanakumar, B. Sakthivel, K. Ravichandran, Simultaneous doping of aluminium and fluorine on zinc oxide nanopowder using a low-cost soft chemical route. *Mater. Lett.* **65**, 2278–2280 (2011)
2. D. Pooja, S.K. Sharma, M. Knobel, R. Rani, M. Singh, Magnetic properties of Fe doped ZnO nanosystems synthesized by solution combustion method, *Res. J. Recent Sci.* **1**, 48–52 (2012)
3. Arooj, S. Nazir, A. Nadhman, N. Ahmad, B. Muhammad, I. Ahmad, K. Mazhar, R. Abbasi, ZnO:Ag nanocomposites induce significant oxidative stress in human fibroblast Malignant

- melanoma (Ht144) cells, Beilstein J. Nanotechnol. **6**, 570–582 (2015)
4. B. Sankara Reddy, S. Venkatramana Reddy, N. Koteeswara Reddy, Y. Prabhakara Reddy, Structural, optical and magnetic properties of (Fe, Ag) co-doped ZnO nanostructures, *Adv. Mater. Lett.* **5**, 199–205 (2014)
 5. S.B. Rana, P. Singh, A.K. Sharma, A.W. Carbonari, R. Dogra, Synthesis and Characterization of pure and doped ZnO nanoparticles. *J. Opto. Electron. Adv. Mater.* **12**, 257–261 (2010)
 6. G. Murugadoss, Synthesis and characterization of transition metals doped ZnO nanorods, *J. Mater. Sci. Technol.* **28**, 587–593 (2012)
 7. M. Caglar, F. Yakuphanoglu, Structural and optical properties of copper doped ZnO films derived by sol–gel method. *Appl. Surf. Sci.* **258**, 3039–3044 (2012)
 8. S. Saravanan, M. Silambarasan, T. Soga, Structural, morphological and optical studies of Ag doped ZnO nanoparticles synthesized by simple solution combustion method. *J. Appl. Phys.* **53**, 1–6 (2014)
 9. R. Mohan, K. Ravichandran, A. Nithya, K. Jothivenkatachalam, C. Ravidhas, B. Sakthivel, Influence of spray flux density on the photocatalytic activity and certain physical properties of ZnO thin films. *J. Mater. Sci: Mater. Electron.* **25**, 2546–2553 (2014)
 10. S. Gayathri, O.S. Nirmal Ghosh, S. Sathishkumar, P. Sudhakara, J. Jayaramudu, S.S. Ray, A. Kasi Viswananath, Investigation of physicochemical properties of Ag doped ZnO nanoparticles prepared by chemical route. *Appl. Sci. Lett.* **1**, 8–13 (2015)
 11. S. Bandyopadhyay, C.K. Paul, R. Roy, S.K. Sen, S. Sen, Study of structural and electrical properties of grain boundary modified ZnO films prepared by sol –gel technique, *Mater. Chem. Phys.* **74**, 83–91 (2002)
 12. K. Saravanakumar, B. Sakthivel, K. Ravichandran, Simultaneous doping of aluminum and fluorine on Zinc oxide nanopowder using a low cost soft chemical route. *Mater. Lett.* **65**, 2278–2280 (2011)
 13. P.K. Labhane, V.R. Huse, L.B. Patle, A.L. Chaudhari, G.H. Sonawane, Synthesis of Cu doped ZnO nanoparticles: crystallographic, optical, FTIR, morphological and photocatalytic study. *J. Mater. Sci. Chem. Eng.* **3**, 39–51 (2015)
 14. S. Thakur, N. Sharma, A. Varkia, J. Kumar, Structural and Optical properties of copper doped ZnO nanoparticles and thin films, *Adv. Appl. Sci. Res* **5**, 18–24 (2014)
 15. T. Ghoshal, S. Biswas, S.K. M. Paul De, Synthesis of ZnO nanoparticles by solvothermal method and their ammonia sensing properties. *J. Nanosci. Nanotechnol.* **9**, 5973–5980 (2009)
 16. K. Karthika, K. Ravichandran, Enhancing the magnetic and antibacterial properties of ZnO nanopowders through Mn + Co doping. *Ceram. Int.* **41**, 7944–7951 (2015)
 17. K. Ravichandran, K. Saravanakumar, R. Chandramohan, V. Nandhakumar, Influence of Simultaneous doping of Cd and F on certain physical properties of ZnO nanopowders synthesized via a simple soft chemical route. *Appl. Surf. Sci.* **261**, 405–410 (2012)
 18. D. Phong pham, K. Khanh Huynh, C. Vinh Tran, V. Quang Vu, Preparation and structural Characterization of Sol–gel-derived silver silica nanocomposite powders. *Int. J. Mater. Sci. Appl.* **3**, 147–151 (2014)
 19. S.B. Rana, P. Singh, A.K. Sharma, A.W. Carbonari, R. Dogra, Synthesis and characterization of pure and doped ZnO nanoparticles. *J. Opt. Electron. Adv. Mater.* **12**, 257–261 (2010)
 20. V. Porkalai, D.Benny Anburaj, B. Sathya, G. Nedunchezian, Effect of calcinations on the structural and morphological properties of Ag and In codoped ZnO nanoparticles. *J. Mater. Sci.* (2016). doi:10.1007/s10854-016-5826-1
 21. S. Kumar, P. Vats, S. Gautam, V.P. Gupta, K.D. Verma, K.H. Chae, M. Hashim, H.K. Choi, Electronic structure, magnetic and structural properties of Ni doped ZnO nanoparticles. *Mater. Res. Bull.* **59**, 377–381 (2014)
 22. M. Saleem, L. Fang, A. Wakeel, M. Rashad, C.Y. Kong, Simple preparation and substrate. *J. Cond. Mater. Phys.* **2**, 10–15 (2012)
 23. I. Kartharinal punithavathy, J. Prince Richard, S. Johnson Jeyakumar, M. Jothibas, P. Praveen, Photodegradation of methyl violet dye using ZnO nanorods. *J. Mater. Sci.* (2016). doi:10.1007/s10854-016-5823-4
 24. S. Muthukumar, R. Gopalakrishnan, Structural, optical and photoluminescence studies of heavily Mn-doped ZnO nanoparticles annealed under Ar atmosphere. *J. Mater. Sci.* **23**, 1393–1401 (2012)
 25. J. Lu, K. Huang, J. Zhu, X. Song, Z. Sun, Preparation and characterization of Na-doped ZnO thin films by sol–gel method. *Physica B* **405**, 3167–3171 (2010)
 26. M. Ram, G.S. Arya, K. Parmar, R.K. Kotnala, N.S. Negi, Structural, Microstructural and raman study of co-doped ZnO nanocrystals synthesized by solution combustion method. *Int. J. Adv. Eng. Technol.* **8**, 329–336 (2015)
 27. S.M. Hosseini, I. Abdolhosseini sarsari, P. Kameli, H. Salamati, Effect of Ag doping on structural, optical, and photocatalytic properties of ZnO nanoparticles. *J. Alloys. Compd.* **640**, 408–415 (2015)
 28. K. Ravichandran, A. Anbazhagan, M. Beneto, N. Dineshbabu, C. Ravidhas, Enhancement of the Hachee’s quality factor of sol–gel spin coated ZnO thin films by MO doping. *Mater. Sci. Semicond. Process.* **41**, 150–154 (2016)
 29. K. Ravichandran, R. Anandhi, K. Karthika, P.V. Rajkumar, N. Dineshbabu, C. Ravidhas, Effect of annealing on the transparent conducting properties of fluorine doped Zinc oxide and tin oxide thin films-A comparative study. *Superlattices Microstruct.* **83**, 121–130 (2015)
 30. S. Snega, K. Ravichandran, M. Beneto, S. Vijayakumar, Simultaneous enhancement of transparent and antibacterial properties of ZnO films by suitable F doping. *J. Mater. Sci. Technol.* **31**, 759–765 (2015)
 31. N. Jabena Begam, K. Ravichandran, Effect of source material on the transparent conducting properties of sprayed ZnO:Al thin films for solar cell applications. *J. Phys. Chem. Solids.* **74**, 841–848 (2013)
 32. T.M. Hammad, J.K. Salem, R.G. Harrison, Structure, optical properties and synthesis of Co-doped ZnO superstructures. *Appl. Nanosci.* **3**, 133–139 (2013)
 33. Z.T. Khodair, A.R. Alarraf, M.I. Manssor, N.A. Bakr, Synthesis and study of ZnO nanorods and Fe-doped ZnO nanoflowers by atmospheric pressure chemical vapour deposition (APCVD) technique. *J. Electron Devices.* **15**, 1200–1208 (2012)
 34. P. Kaur, S.K. Pandey, S. Kumar, N.S. Negi, C.L. Chen, S.M. Rao, Tuning ferromagnetism in Zinc oxide nanoparticles by chromium doping. *Appl. Nano Sci* **5**, 975–981 (2015)
 35. M. Ram, G.S. Arya, K. Parmar, R.K. Kotnala, N.S. Negi, Structural, Microstructural and Raman study of co-doped ZnO nanocrystals synthesized by solution combustion method. *Int. J. Adv. Eng. Technol.* **8**, 329–336 (2015)
 36. S. John Kennady Vethanathan, S. Perumal, S. Meenakshi Sundar, D. Priscilla koilpillai, S. Karpagavalli, A. Suganthi, Optical and structural characterization of Mn and cu doped ZnO nanoparticles. *Int. J. Adv. Sci. Technol. Res.* **2**, 306–319 (2014)
 37. M. Silambarasan, S. Saravanan, T. Soga, Raman and photoluminescence studies of Ag and Fe doped ZnO nanoparticles. *Int. J. Chem Technol. Res.* **7**, 1644–1650 (2015)
 38. T. Marimuthu, N. Anandhan, G. Ravi, S. Rajendran, Structural, functional and optical studies on ce doped ZnO nanoparticles. *J. Nanosci. Nanotechnol.* **2**, 62–65 (2014)
 39. K. Ravichandran, M. Vasanthi, K. Thirumurugan, K. Karthika, B. Sakthivel, Improving the electrical, magnetic and antibacterial

- properties of sol–gel spin coated ZnO thin films through (Sn + Mn) co-doping. *J. Mater. Sci.* **26**, 5451–5458 (2015)
40. K. Ravichandran, R. Rathi, M. Beneto, K. Karthika, P.V. Rajkumar, B. Sakthivel, R. Damodaran, Effect of Fe+ F doping on the antibacterial activity of ZnO powder. *Ceram. Int.* **41**, 3390–3395 (2015)
 41. K. Ravichandran, M. Vasanthi, K. Thirumurugan, B. Sakthivel, K. Karthika, Annealing induced reorientation of crystallites in Sn doped ZnO films. *Opt. Mater.* **37**, 59–64 (2014)
 42. A.S. Menon, N. Kalarikkal, S. Thomas, Studies on structural and optical properties of ZnO and Mn-doped ZnO nanopowders. *Ind. J. Nano Sci.* **1**, 16–24 (2013)